Binary Sequential Ranging With Sine Waves

W. L. Martin and J. W. Layland
Communications Systems Research Section

Current ranging systems of the Deep Space Network estimate the range to a spacecraft by measuring the phase of a square-wave range code after its round-trip from station to spacecraft and back. Distortion of this waveform, in the form of phase-shifts of the harmonics of the square wave, can seriously degrade ranging accuracy. In this report, we show that such degradation can be largely eliminated by zonal filtering the range code to only its sine-wave fundamental at no net cost in ranging signal power or accuracy.

I. Introduction

Current ranging systems of the Deep Space Network estimate the distance from the DSN Tracking Stations to a spacecraft by transmitting to the spacecraft a square-wave range code of approximately 2 μs period, and then measuring the phase of this square wave as it is returned from the spacecraft relative to a time-delayed and doppler-shifted copy of transmitted code (Ref. 1). The ambiguity inherent in the periodicity of this square wave is resolved by using lower frequency codes which are coherent with it. There is currently some interest in increasing the precision to which this measurement is performed, or at least in ensuring that the degree of precision of which the system is theoretically capable is achieved in practice. This article proposes a minor change to existing-type ranging systems which can help to achieve that goal.

Figure 1 is an overall functional block diagram of the ranging operation. The delay through the station alone is measured via the zero-delay or calibration subsystem. The delay through the spacecraft transponder is separately measured prior to flight. The net delay through the transmission medium, from which is inferred the true range, is estimated as the delay value remaining when the station and spacecraft delays are subtracted from the overall measured delay. We are in all cases not measuring the delay per se, but are instead measuring the phase of the square-wave range code. The exact relationship between the measured phase of any nonsinusoidal waveform and its "delay" can be somewhat fuzzy. This fuzziness results if waveform dispersion occurs anywhere along the signal path. We can combat it by using only a sine wave for the highest frequency code component, or by performing all measurements using only the sine wave fundamental of this component. In the following, we review some of the ramifications of this possible change to the binary coded sequential ranging systems.

II. Additive Noise Effects

Let us presume that we wish to use only the fundamental sine wave component of a range code for delay measurement. The first thing to determine is what effect

this will have on the measurement errors due to noise. The signal received, $r(t)$, is assumed to be an ideal square wave, of power s, and delay-shift θ, plus a White noise component $n(t)$ with one-sided spectral density N_0. The reference signal is an ideal unit-amplitude (unit-energy) square wave, and correlation detection is employed at two reference phases to estimate θ. The two correlations obtained are

$$X = \int_0^t SQ_T(\eta) \cdot r(\eta) d\eta$$
$$Y = \int_0^t SQ_T\left(\eta - \frac{T}{2}\right) \cdot r(\eta) d\eta \tag{1}$$

In Eq. 1, t is the measuring integration time and T is the bit period of the code. The expected value of X and Y has peak value $\sqrt{s} \cdot t$ and depends upon θ as shown in Fig. 2. The variance of both X and Y is $N_0 \cdot \frac{t}{2}$. The estimated delay, $\hat{\theta}$ is given by

$$\hat{\theta} = \frac{Y}{|X| + |Y|} \cdot \frac{T}{2} \tag{2}$$

whenever X is positive. Following Goldstein (Ref. 1) we use

$$\sigma_\theta^2 \approx \left(\frac{\partial\theta}{\partial\hat{x}}\right)^2 \sigma_x^2 + \left(\frac{\partial\theta}{\partial\hat{y}}\right)^2 \sigma_y^2 \tag{3}$$

which implies

$$\sigma_\theta^2 \approx \frac{N_0}{2} t \left(\frac{T}{2\sqrt{st}}\right)^2 \left\{\left(1 - \frac{|Y|}{|X| + |Y|}\right)^2 + \left(\frac{-Y \operatorname{sgn} X}{|X| + |Y|}\right)^2\right\}$$
$$\sigma_\theta^2 \leq \frac{N_0 T^2}{8 s t}$$
$$\sigma_\theta^2 \geq \frac{N_0 T^2}{16 s t} \tag{4}$$

The estimator variance is at its maximum when either X or Y is zero, and at its minimum when $|X| = |Y|$. Equation 4 will be our reference against which the variance of the estimated phase of a modified range code will be measured.

As an alternate technique, let us use unit-energy sinusoids for the reference signals. The two correlations obtained are

$$X' = \int_0^t \sqrt{2} \sin\left(\frac{\pi}{T}\eta\right) r(\eta) d\eta$$
$$Y' = \int_0^t \sqrt{2} \cos\left(\frac{\pi}{T}\eta\right) r(\eta) d\eta \tag{5}$$

As before, the variance of both X' and Y' is $N_0 \cdot t/2$. The mean values of X' and Y' will be determined by expanding the received square-wave range code in its Fourier series form.

$$r(\eta) = n(\eta) + \sqrt{s} \cdot \frac{4}{\pi} \cdot \sum_{i \text{ odd}} \frac{1}{i} \sin\left[i \cdot \frac{\pi}{T} \cdot (\eta + \theta)\right] \tag{6}$$

The two correlations are then approximately given by

$$X' = \sqrt{2s} \cdot t \cdot \frac{2}{\pi} \cdot \cos\left(\frac{\pi}{T} \cdot \theta\right) + n_x$$
$$Y' = \sqrt{2s} \cdot t \cdot \frac{2}{\pi} \cdot \sin\left(\frac{\pi}{T} \cdot \theta\right) + n_y \tag{7}$$

The estimate of θ is now given by

$$\theta = \frac{T}{\pi} \arctan(Y,X)$$

Using the same technique as before in Eq. 2-4, we find

$$\sigma_\theta^2 = \frac{N_0}{2} \cdot t \cdot \left(\frac{T}{\pi}\right)^2 \Big/ \left[\left(\sqrt{2s}\, t \cdot \frac{2}{\pi}\right)^2 (\sin^2\theta + \cos^2\theta)\right]$$
$$\sigma_\theta^2 = \frac{N_0 T^2}{16 s t} \tag{8}$$

This surprising result indicates that by using only the fundamental component of the received range code, we achieve the same performance with respect to additive noise that we could achieve with the entire square wave, and we achieve such performance irrespective of the actual delay between the received and reference code waveforms. Clearly the harmonics of the square-wave range code are of no benefit to us for conventional ranging operation. They can in fact be detrimental as we shall see shortly.

III. Harmonic Phase-Shift Effects

To understand the effects that harmonic phase shifts, or waveform dispersion, have upon the ranging operation, we need to refer to the overall system diagram of Fig. 1. The calibration-subsystem in the station is wideband and as close to delay-free as possible. As a result, when range measurement is performed in-station to calibrate station equipment delays, it is almost entirely the station equipment, the receiver, the exciter, modulator, and transmitter, and the ranging subsystem itself that establishes the details of the range code waveform, and its harmonic structure. The spacecraft transponder, on the other hand, has a limited bandwidth that passes only the fundamental and its third harmonic; in current transponders, the third harmonic is somewhat attenuated, although not phase-shifted.

The range to the spacecraft is measured as follows: first, the station delay is measured, with all station equipment in the configuration which will be used with the spacecraft measurement. Next, the delay is measured through the Earth-to-spacecraft link and the spacecraft transponder, and then the station delay and the previously measured spacecraft delay are subtracted from this value. (See Ref. 2 for more detail.) For error-accounting, the calibration subsystem is directly in the range-measurement path. We envision two cases: first, where the station equipment generates and processes a perfect square wave range code, and second, where some station equipment has changed in such a way that the harmonics of the range code are phase-shifted and/or attenuated relative to the fundamental. For both cases, the spacecraft transponder passes first and third harmonics of the range code with no relative phase shift, although with some, say 3 dB, attenuation of the third harmonic. Additive noise will be ignored.

The range code received at the ranging subsystem via the station's receiver may be represented as

$$r(t) = \frac{4}{\pi}\left\{\sin\left(\frac{\pi}{T}t\right) + \frac{\alpha_3}{3}\sin\left(3\frac{\pi}{T}\cdot t + \theta_3\right) + \frac{\alpha_5}{5}\sin\left(5\frac{\pi}{T}\cdot t + \theta_5\right) + \cdots\right\} \tag{9}$$

where we denote by α_k/k, the gain, and θ_k, the phase shift of the kth harmonic relative to the first. The two correlation values used to compute the delay value are

$$X(\tau) = C\cdot\left\{\cos\left(\frac{\pi}{T}\tau\right) + \sum_{\substack{k=3\\ odd}}^{\infty}\frac{\alpha_k}{k^2}\cos\left(k\cdot\frac{\pi}{T}\cdot\tau + \theta_k\right)\right\}$$
$$Y(\eta) = X(\eta - T/2) \tag{10}$$

During most of its operation, the local code reference of the ranging subsystem is constrained to track so that $X(\tau) = Y(\tau)$, and the real delay measurement is contained within the physical shifts accumulated by the local coder. This forces

$$0 \equiv X(\tau) - X(\tau - T/2)$$
$$0 \equiv \left\{\cos\left(\frac{\pi}{T}\cdot\tau\right) - \cos\left(\frac{\pi}{T}\cdot\tau - \frac{\pi}{2}\right)\right\} + \sum_{\substack{k=3\\ odd}}^{\infty}\frac{\alpha_k}{k^2}\left\{\cos\left(k\cdot\frac{\pi}{T}\cdot\tau + \theta_k\right) - \cos\left(k\cdot\frac{\pi}{T}\cdot\tau + \theta_k - \frac{\pi}{2}\right)\right\} \tag{11}$$

The true tracking point is at $\tau = T/4$. If we define η as the offset from the true tracking point, i.e., $\eta = \tau - T/4$, change variables in Eq. (11), and manipulate it with trigonometric identities, the tracking point is defined by:

$$0 \equiv \sin\left(\frac{\pi}{4}\right)\cdot\sin\left(\frac{\pi}{T}\eta\right) + \sum_{k=3,\text{odd}}^{\infty}\frac{\alpha_k}{k_2}\sin\left(k\frac{\pi}{4}\right)\cdot\sin\left(k\cdot\frac{\pi}{T}\eta + \theta_k\right) \tag{12}$$

or

$$0 \equiv \sin\left(\frac{\pi}{4}\right)\cdot\sin\left(\frac{\pi}{T}\eta\right) + \sum_{k=3,\text{odd}}^{\infty}\frac{\alpha_k}{k^2}\sin\left(k\frac{\pi}{4}\right)\cdot\left\{\sin\left(k\cdot\frac{\pi}{T}\eta\right)\cdot\cos(\theta_k) + \cos\left(k\cdot\frac{\pi}{T}\eta\right)\cdot\sin(\theta_k)\right\}$$

Denoting by $\lceil x\rceil$, the greatest integer less than x, we can represent $\sin\left(k\frac{\pi}{4}\right) = \sin\left(\frac{\pi}{4}\right)\cdot(-1)^{\lceil k/4\rceil}$ for all odd k. Let us also assume that η is small; that for any offset which is of genuine interest with respect to ranging, we can approximate

$$\sin\left(k\cdot\frac{\pi}{T}\cdot\eta\right) \approx k\cdot\frac{\pi}{T}\eta$$
$$\cos\left(k\cdot\frac{\pi}{T}\cdot\eta\right) \approx 1 \tag{13}$$

Then the offset from the true tracking position is given by

$$\eta \approx -\frac{T}{\pi}\frac{\sum \frac{\alpha_k}{k^2}(-1)^{\lceil k/4\rceil}\sin\theta_k}{1+\sum \frac{\alpha_k}{k}(-1)^{\lceil k/4\rceil}\cos\theta_k} \tag{14}$$

Note that there are two obvious conditions which can make $\eta = 0$: if either $\theta_k = 0$, for all k, or if $\alpha_k = 0$, for all $k \geq 3$. In both cases, the delay measured by the ranging system is the delay suffered by the range code fundamental and there is no fuzziness in the meaning of that delay. The second case corresponds to performing the range measurement with the code fundamental only.

The details of the error in the ranging operation can now be determined. If the station equipment generates and processes a perfect square wave, then there is no error caused by the code harmonics in measuring station delays, and $\eta = 0$. Similarly, even though the transponder filters out harmonics so that $\alpha_k \simeq 0$ for $k \geq 5$, and $\alpha_3 < 1$, we still have $\theta_3 = 0$ so that $\eta = 0$ in measuring delays through the spacecraft also. If we have also a calibration of the spacecraft delays using a perfect square wave, the net error in measuring range to that spacecraft is nil.

In an alternate scenario, let us assume that some harmonic distortion arises somewhere within the complex equipment of the tracking station. The delay measured for the ground system then suffers an error which is well described by Eq. (14). Let β_3 be the gain factor of the spacecraft alone at the third harmonic of the high frequency range code, and use $\beta_k = 0$ for $k \geq 5$ to indicate that the transponder does not pass the fifth and higher harmonics. Assume that the spacecraft adds no phase shift to the third harmonic, and let α_k, θ_k as before denote station equipment amplitude and phase characteristics. Then the delays measured through the spacecraft are in error by

$$\eta_{s/c} = -\frac{T}{\pi}\frac{\frac{1}{9}\alpha_3\beta_3\sin\theta_3}{1+\frac{1}{3}\alpha_3\beta_3\cos\theta_3} \tag{15}$$

And if we assume that the spacecraft delay itself was calibrated with a reference station without distortion, the net error in measuring spacecraft range is $\eta_{s/c} - \eta$, or

$$RE = \frac{T}{\pi}\left\{\frac{\sum \frac{\alpha_k}{k^2}(-1)^{\lceil k/4\rceil}\sin\theta_k}{1+\sum \frac{\alpha_k}{k}(-1)^{\lceil k/4\rceil}\cos\theta_k} - \frac{\frac{1}{9}\alpha_3\beta_3\sin\theta_3}{1+\frac{1}{3}\alpha_3\beta_3\cos\theta_3}\right\} \tag{16}$$

For a concrete example, consider a station system which has $\alpha_3 = \alpha_5 = 1$, $\alpha_k = 0$ for $k \geq 7$, and has $\theta_3 = 10$ deg, $\theta_5 = -30$ deg, and a spacecraft for which $\beta_3 = 1/2$. Here, the resultant range error is

$$RE = \frac{T}{\pi} \times \left\{\frac{\frac{1}{9}\sin 10\text{ deg} + \frac{1}{25}\sin 30\text{ deg}}{1+\frac{1}{3}\cos 10\text{ deg} - \frac{1}{5}\cos 30\text{ deg}} - \frac{\frac{1}{18}\sin 10\text{ deg}}{1+\frac{1}{6}\cos 10\text{ deg}}\right\} \tag{17}$$

$$RE = .008 * T$$

In current ranging systems, where T is approximately one microsecond, this resultant error is eight nanoseconds, or approximately 2-1/2 meters. Larger errors than this are quite plausible, considering the amount of equipment in the ranging signal path!

IV. Ameliorating the Waveform Dispersion Effects

There are a number of alternative things which can be done in response to the magnitude of the effects evidenced in Eq. (16). First of all, if the overall error budget is of the order of 10 to 20 meters, it can simply be ignored, as reasonable care with the equipment can restrain RE well below this value. If, however, we are asking how accurate the spacecraft range can be measured, then more care must be used. As a second approach, we could design and control the parameters of all tracking stations of the Network so that phase-shifts imposed upon the harmonics of range code by the station equipment are held within

prespecified tolerances. The actual phase-shift tolerances allowable may be determined from Eq. (16) once the allowable range-error is established. A third alternative is to make the calibration subsystem itself mimic the transfer characteristics of the spacecraft transponder. In this way, the harmonic structure of the range code arriving at the ranging subsystem via either the spacecraft or the calibration subsystem is identical, and the range error equation analogous to Eq. (16) is likewise ideally zero. Considering component tolerances, and in particular, variations between spacecraft transponders, there would in fact be some slight residual range error resulting.

The fourth alternative is that one which is being promulgated by this report, namely the use of the fundamental sine wave component only of the range code. This can be accomplished by inserting an appropriate filter anywhere on the signal path within the station equipment that is common to both the spacecraft and calibration measurements, or by use of a sine-wave reference waveform as was analyzed in part II. Use of the sine-wave reference seems impractical from the standpoint of available equipment. Appropriate filtering of the received signal on the path from the receiver to the ranging subsystem can achieve the identical result. Filtering at the receive-end of the signal path will remove all coherent harmonics of the range code, not only those generated intentionally as part of the square-wave range code, but also those which arise from nonlinearities along the signal path. Filtering could also be applied to the uplink range code between the ranging subsystem and the modulator. If the average uplink modulation index is maintained, and no peak deviation limit is imposed, the ranging signal power is in fact slightly increased. Filtering of the uplink, however, does not eliminate the desirability of further filtering of the downlink, since nonlinearities in the ranging path beyond the uplink filter can still inject harmonics at strange phase-angles. The filter (or filters) are directly in the group-delay path of the ranging measurement and their delay stability is critical to range accuracy, even though the exact delay value is not.

For the experiments to be described, the filter was inserted in the 10-MHz signal line from the receiver as shown in Fig. 3. This point is preferable to others since it is the last opportunity to remove distortion prior to correlation and therefore serves to offset any degradation occurring elsewhere in the system. In principle, a correlator using a pure sine-wave reference would be superior. However, because the present systems are all mechanized using digital techniques the external filter was selected as the most practical approach.

The characteristics of the filter needed to be uniform across the band pass with a linear phase-frequency slope so as to ensure maximum group delay stability. However, once the band edge was reached, a rapid attenuation was desired to eliminate unwanted harmonics. It was decided to design for a cutoff frequency of ± 1 MHz and a rejection of at least 60 dB in the stop band beyond ± 1.5 MHz where the offending harmonics are located.

A schematic diagram of the filter is shown in Figure 4 (component values will be found in Table 1). An elliptic function design was selected as providing the best band-pass relative to band-stop characteristics. While ripples exist both within and without the band pass, their magnitude is sufficiently small that the performance of the filter should not be affected. Moreover, the steep attenuation characteristic obtainable with this design makes its use in this application attractive.

The basic design consists of a low-pass filter, 1 MHz in bandwidth which has been translated to 10 MHz by resonating elements. Because certain, identifiable, components determine the attenuation characteristics while others control center frequency and symmetry, it is important to select these critical components carefully.

For example, L1 to L4 and C5 to C11 comprise the basic low-pass filter and therefore determine the band-pass/band-stop characteristics as well as the transition between. Because the placement of poles and zeros is critical to this design, it is important that actual component values be selected to accurately reflect the computed numbers. The procedure followed with inductors was to adjust the number of turns with the aid of an inductance bridge until the closest possible value was obtained. Using this method, inductances within one percent of the calculated values could be realized. With the capacitors, up to three were connected in parallel to bring the capacitance to within one percent of the computed value.

Because of the high performance requirements and the critical characteristics of this filter noted earlier, it was necessary to utilize high Q circuit components. Glass capacitors were used throughout and the torroidal inductors were wound with the largest size wire which could reasonably be fitted on the ferrite cores. Measured Q's for the finished inductors were in excess of 100.

After collecting the components comprising the low-pass portion of the filter, it was necessary to translate the entire spectrum to a 10-MHz center frequency for use

with the ranging system. This was accomplished with C1 to C4 and L5 to L11. Since the only purpose of these components is to adjust the center frequency, conformance with calculated values is less important. The procedure followed was to pick an element within the low-pass filter and adjust the translating component so that the pair was resonant at 10 MHz. Thus C1 was trimmed until L1 and C1 were a series tuned circuit at 10 MHz. Likewise, turns were changed on L8 until it formed a parallel tuned circuit with C8. In general, each of the 11 tuned circuits (Ln, Cn) comprising the filter was adjusted individually.

The element pairs were then assembled into a specially made copper module as shown in Figure 5. Because of the high attenuation required, it was deemed advisable to separate the various sections into four compartments to minimize leakage. An effort was made to place the components in the center of the cell to reduce stray capacitance; the module itself served as circuit ground.

Following assembly, tests were made to determine the bandwidth of the filter, and group delay and phase delay characteristics. Figure 6 is a photograph of the amplitude response as measured with a General Radio model 1711 Sweep Generator and associated Model 1714 Display Unit. A sweep speed of 500 kHz per centimeter was used so as to provide maximum resolution in the frequency band from 8 through 12 MHz.

The response appears to be reasonably symmetrical about the 10-MHz center frequency particularly at ± 500 kHz where the first range code sidebands are located. Beyond approximately ± 900 kHz the filter begins to reduce the signal rapidly. At ± 1.5 MHz where the third range code harmonic is situated, the attenuation exceeds 60 dB. While there is a slight asymmetry on the high frequency side of the curve, between about 1.2 and 1.4 MHz, it is considered unimportant since the design goal had been met at the ± 1.5 MHz frequencies.

Figure 7 shows the phase delay over the same band of frequencies. Because of the measurement technique, the figure appears to have a sawtooth pattern. In fact, the heavier lines, sloping down to the right, should be treated as a single continuous, unsegmented line. Ideally, the phase change should be linear with varying frequency. Practically, this is difficult to obtain in a multipole filter such as this one. In this case, the phase-frequency relationship is reasonably linear over a range sufficient to contain the first range code sidebands. Since the code spectrum is discrete, nonlinearities occurring beyond 10 MHz ± 500 kHz should not materially affect the group delay.

Filter group delay appears in Figure 8. Note that the filter has an insertion delay of approximately 600 nanoseconds at 10 MHz. This increases to about 700 nanoseconds for the lower range code sideband (9.5 MHz) and to about 900 nanoseconds for the upper sideband (10.5 MHz). The average sideband delay compares well with the 808 nanosecond delay actually measured by the ranging system.

At this point the intrinsic problem with filters is obvious. Where large attenuations and steep transitions are required, a design meeting these conditions will also include a rather substantial group delay. With large delays come the concomitant problems with stability which may introduce errors considerably in excess of those sought to be eliminated. The underlying problem, of course, is one of trying to resolve a phase comparison to approximately 0.1 percent. Clearly, this defect could be substantially reduced by widening the bandwidths and raising the code frequency. However, since the intent here was merely to investigate the feasibility of a filter as a solution to the harmonic phase shift problem, little attention was devoted to stabilizing the unit for field operations.

V. Ranging Test Results

To test the effectiveness of the filter as well as the hypothesis that much of the ranging inaccuracy is caused by nonuniform phase shifts in the higher order range code harmonics, the system was connected as shown in Figure 3. First, the system delay was measured using a zero delay device. Second, a Mariner Venus-Mercury transponder was substituted for the zero delay device and the total delay remeasured. The difference between this and the prior measurement represents the transponder delay. Thereafter, the phase modulator in the ground exciter system was changed and the entire procedure repeated. In principle, the transponder delay should remain unchanged. However, because of the way in which the modulator and spacecraft ranging channel act upon the higher order range code harmonics, the transponder delay undergoes an apparent change. Installation of the filter served to remove the range code harmonics so that correlation is only with the code fundamental.

Results of these tests are shown in Figure 9. Transponder delays were measured at 1-dB and 9-dB carrier suppression. Two ground system modulators were employed. Number 2002 exhibited fairly normal operating characteristics. However, number 2034, while allegedly meeting Network test specifications, had been observed to exhibit unusual behavior such as low sensitivity.

It can be seen from the figure that the transponder delay varies greatly as the modulation index is changed on number 2034. This distortion is substantially greater at low modulation levels than it is at high levels. Note that with the filter installed, the difference is reduced to less than one-third of its former value at small modulation angles. As the carrier suppression is increased to 9 dB the differences have disappeared within the uncertainty of the measurement as indicated by the brackets. However, while making a dramatic improvement, the effect is still present. Since it seems unlikely that any higher order harmonics are passing through the filter, the explanation must lie elsewhere. At this juncture it is uncertain why divergence exists and further tests will be necessary to develop a better understanding of the causal relationships.

VI. Summary and Future Plans

Our preliminary analysis, described herein, has confirmed the existence of a real, or at least a potential, limitation to ranging accuracy resulting from phase shifts of the higher harmonics of the square-wave range code. Experimental and analytical evidence has been developed which shows that this limitation can be largely eliminated by filtering the range code to its fundamental component only at the receiver.

Additional testing should be performed to more exactly quantify the improvement to be obtained in this manner. Also, since that filter is now itself a critical component of the station's group delay path, the stability of that filter under temperature and other environmental variables must be determined.

Acknowledgment

Experimental results reported herein were cbtained with the able and gracious assistance of Mr. D. L. Brunn, and the staff of the Telecommunications Development Laboratory.

References

1. Goldstein, R. M., "Ranging with Sequential Components," JPL SPS-37-52, Vol. II, pp. 48-49, July 31, 1968.

2. Otoshi, T. Y. and Batelaan, P. D., "S/X Band Experiment: Zero Delay Device," JPL *DSN Progress Report* 32-1526, Vol. XIV, pp. 73-80, April 15, 1973.

Table 1. Filter components

Component designation	Computed value	Measured value	Measured Q
L1	5.11 μH	4.95 μH	185
L2	4.17 μH	4.27 μH	195
L3	5.09 μH	4.90 μH	195
L4	4.75 μH	4.60 μH	195
L5	0.792 μH	0.790 μH	185
L6	0.259 μH	0.262 μH	185
L7	0.395 μH	0.400 μH	175
L8	0.157 μH	0.157 μH	140
L9	0.115 μH	0.116 μH	130
L10	0.137 μH	0.136 μH	130
L11	0.127 μH	0.126 μH	140
C1	50 pF	50 pF	
C2	60.7 pF	61 pF	
C3	49.7 pF	50 pF	
C4	53 pF	53 pF	
C5	320 pF	320 pF	
C6	977 pF	980 pF	
C7	641 pF	640 pF	
C8	1612 pF	1612 pF	
C9	2198 pF	2200 pF	
C10	1849 pF	1847 pF	
C11	1989 pF	1980 pF	

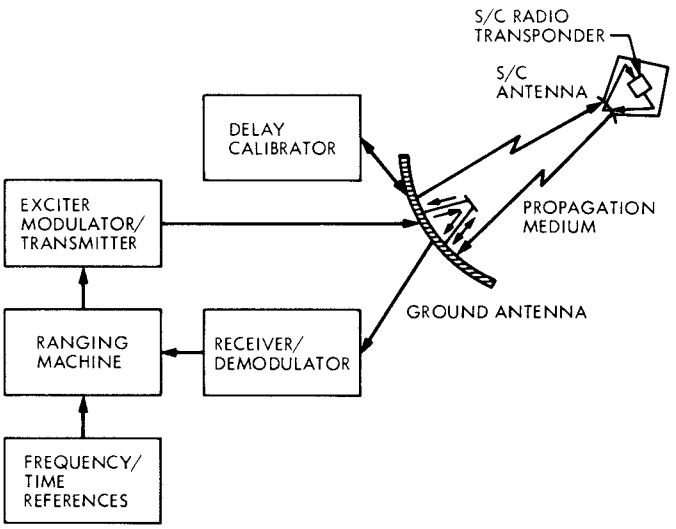

Fig. 1. System block diagram

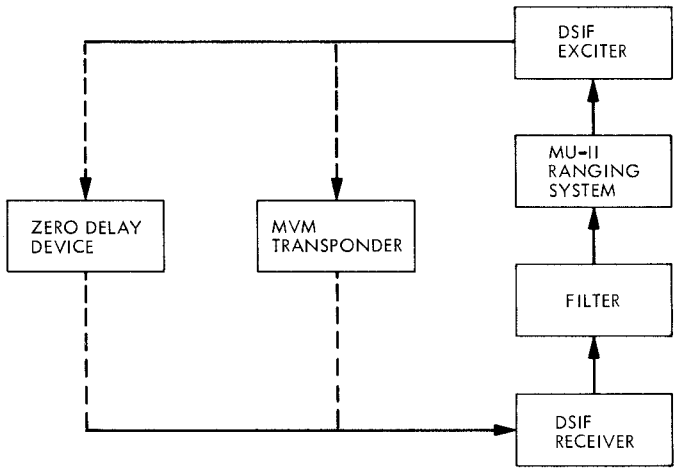

Fig. 3. Filter test configuration

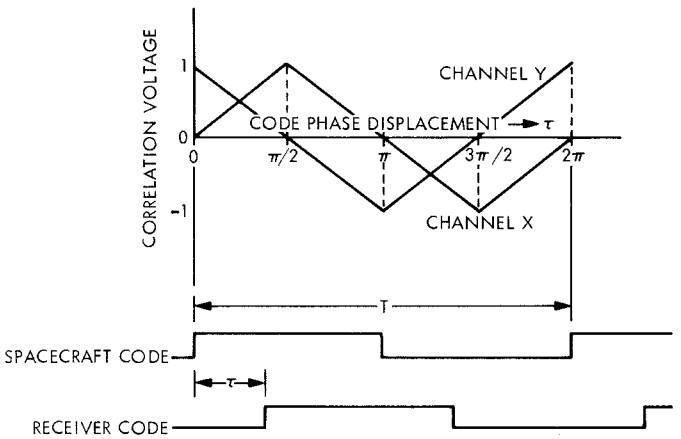

Fig. 2. Ranging correlation values for square-wave reference

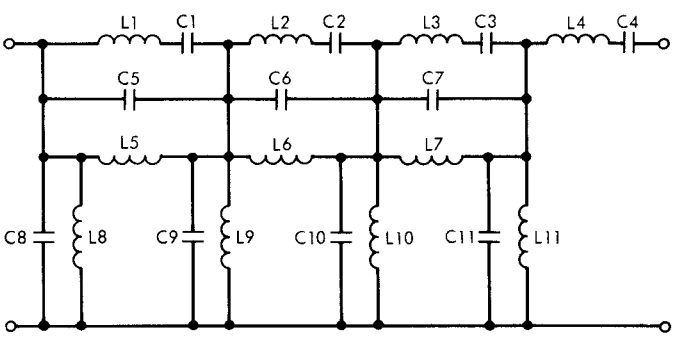

Fig. 4. Ranging code filter schematic

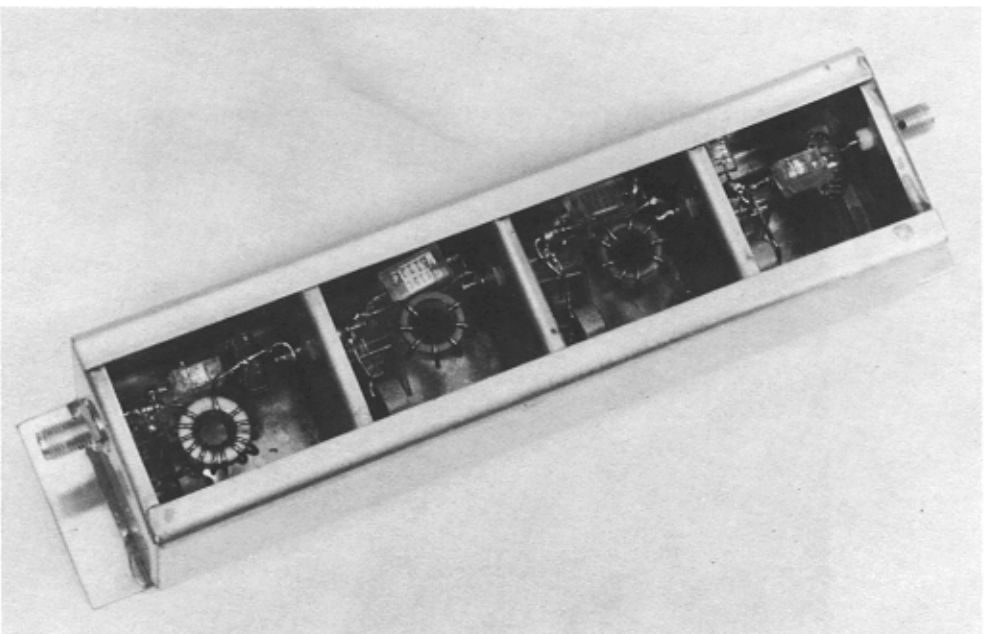

Fig. 5. Ranging code filter module

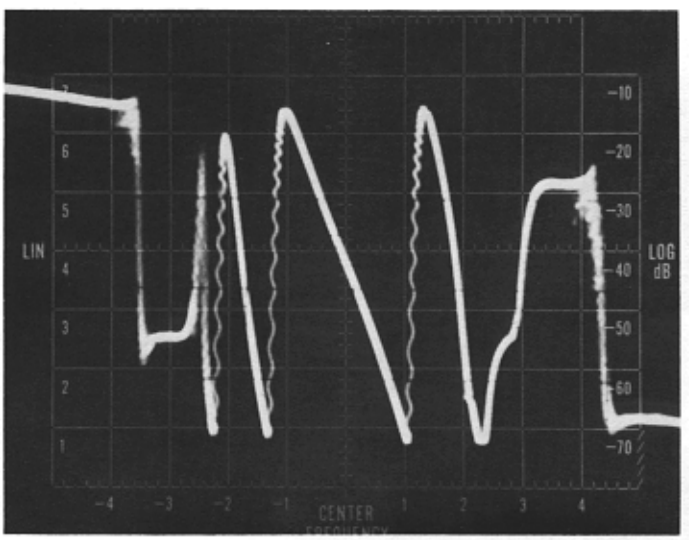

SWEEP SPEED. HORIZ. 500 KHz per cm
VERT. 50 deg per cm

CENTER FREQUENCY 10 MHz

Fig. 6. Filter amplitude response

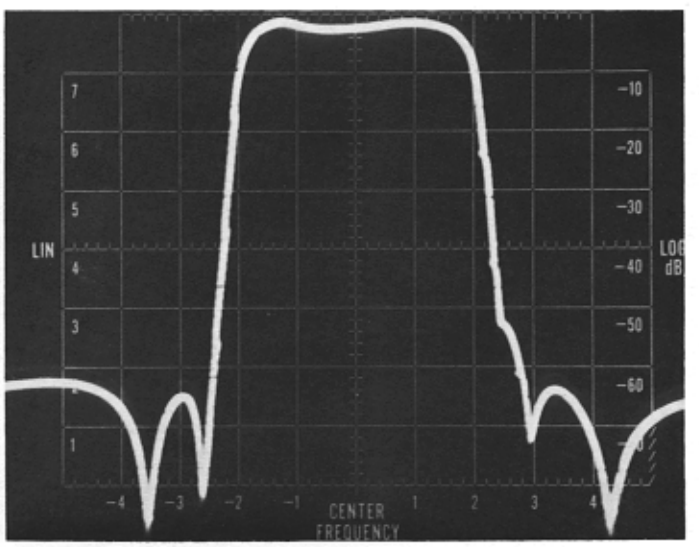

SWEEP SPEED: HORIZ. 500 kHz per cm
VERT. 10 dB per cm

CENTER FREQUENCY 10 MHz

Fig. 7. Filter phase delay

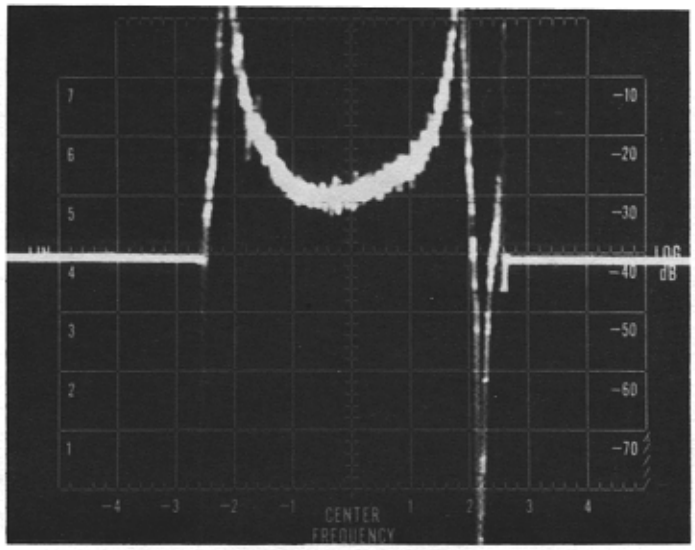

SWEEP SPEED. HORIZ. 500 KHz per cm
VERT. 500 ns per cm

CENTER FREQUENCY 10 MHz

Fig. 8. Filter group delay

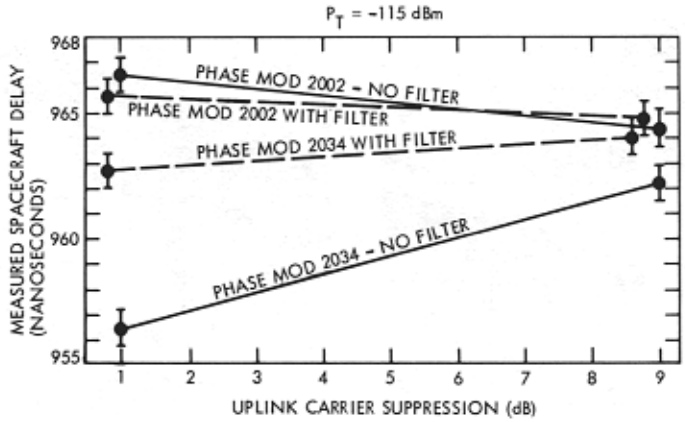

Fig. 9. Filter insertion results